Title

Mechanistic Investigations of Human Reticulocyte 15- and Platelet 12-Lipoxygenases with Arachidonic Acid

Journal

Biochemistry, 48(26)

ISSN

0006-2960

Authors

Wecksler, Aaron T

Jacquot, Cyril

van der Donk, Wilfred A

et al.

Publication Date

2009-07-07

DOI

10.1021/bi802332j

Published in final edited form as:
Biochemistry. 2009 July 7; 48(26): 6259–6267. doi:10.1021/bi802332j.

Mechanistic Investigations of Human Reticulocyte 15- and Platelet 12-Lipoxygenases with Arachidonic Acid†

Aaron T. Wecksler[1], **Cyril Jacquot**[2], **Wilfred A. van der Donk**[2,*], and **Theodore R. Holman**[1,*]

[1]Chemistry and Biochemistry Department, University of California, Santa Cruz, Santa Cruz, CA 95064, Phone 831-459-5884, FAX 831-459-2935

[2]Department of Chemistry, University of Illinois at Urbana-Champaign, 600 South Mathews Ave., Urbana, Illinois 61801, Phone 217-244-5360, FAX 217-244-8068

Abstract

Human reticulocyte 15-lipoxygenase-1 (15-hLO-1) and human platelet 12-lipoxygenase (12-hLO) have been implicated in a number of diseases, with differences in their relative activity potentially playing a central role. In the current paper, we characterize the catalytic mechanism of these two enzymes with arachidonic acid (AA) as the substrate. Using variable-temperature kinetic isotope effects (KIE) and solvent isotope effects (SIE), we demonstrate that both k_{cat}/K_m and k_{cat} for 15-hLO-1 and 12-hLO involve multiple rate-limiting steps that include a solvent dependent step and hydrogen atom abstraction. Nevertheless, an unexpectedly low k_{cat}/K_m KIE was determined for 15-hLO-1 (KIE = 8), which increases to well above semi-classical predictions (KIE = 18) upon the addition of the allosteric effector molecule, 12-hydroxyeicosatetraenoic acid (12-HETE), indicating a tunneling mechanism. Furthermore, the addition of 12-HETE lowers the observed k_{cat}/K_m SIE from 2.2 to 1.4, indicating that the rate-limiting contribution from solvent rearrangement in the reaction mechanism of 15-hLO-1 has decreased, with a concomitant increase in the C-H abstraction contribution. Finally, the allosteric binding of 12-HETE to 15-hLO-1 decreases the $K_m(O_2)$ for AA, but increases the $K_m(O_2)$ for LA, such that the $K_m(O_2)$ values become similar for both substrates (~20 μM). Considering that the oxygen concentration in cancerous tissue can be below 5 μM, this result may have cellular implications with respect to the substrate specificity of 15-hLO-1.

Keywords

lipoxygenase; arachidonic acid; kinetic isotope effect; solvent isotope effect

In the human cell, the hydroperoxidation of polyunsaturated fatty acids using molecular oxygen is accomplished by the human lipoxygenase (hLO) isozyme family (Scheme 1) (1). 5-hLO, 12-hLO and 15-hLO are the three main lipoxygenases in the cell and are named according to their positional specificity on arachidonic acid (AA), producing their respective hydroperoxyeicosatetraenoic acid (HPETE) products. The LO products are responsible for inflammatory response, but they are also implicated in a variety of other human diseases. 5-hLO is involved in asthma (2) and cancer (3,4), 12-hLO is involved in psoriasis (5) and cancer (4,6,7) and 15-hLO is involved in atherosclerosis (8) and cancer (4,9).

†This work was supported by the National Institutes of Health (GM44911, WAV and GM56062, TRH) and an American Heart Association pre-doctoral fellowship (0615604Z, CJ).

*Authors to which all inquiries should be addressed, tholman@chemistry.ucsc.edu, vddonk@uiuc.edu.

Recently, the substrate specificity of the 15-hLO isozymes has been suggested to play a role in prostate cancer since their respective products have different cellular responses (10-12). Reticulocyte 15-hLO-1 and epithelial 15-hLO-2 react with both LA and AA, although 15-hLO-1 reacts preferentially towards LA, while 15-hLO-2 reacts preferentially towards AA. However, this substrate specificity is highly dependent on the reaction conditions, such as the detergent used (13-15). In addition, the substrate specificity of both 15-hLO-1 and 15-hLO-2 can be affected by product binding to the allosteric site, suggesting an auto-regulatory mechanism (13). In contrast, 5-hLO and platelet 12-hLO are more selective and only react with AA. For comparison, soybean lipoxygenase-1 (sLO-1), a plant homologue and model enzyme for 15-hLO-1, also reacts preferentially with AA over LA (13,16), even though AA is not a native substrate in soybeans.

Regarding the mechanism by which these lipoxygenases oxygenate fatty acids, LOs are purified in the inactive Fe(II)-OH_2 form and are activated to the Fe(III)-OH form by the hydroperoxide product, resulting in an observable kinetic lag phase (Scheme 1). A hydrogen atom is abstracted from the 1, 4-diene, forming a Fe(II)-OH_2/ pentadienyl radical intermediate. Oxygen attacks the pentadienyl radical and the Fe(II)-OH_2 reduces the hydroperoxide radical to form the product, leaving the active Fe(III)-OH species (1). The kinetics of this reaction with sLO-1 has been extensively studied and with LA as the substrate, the low temperature k_{cat}/K_m[LA] has three rate-determining steps (RDS's) consisting of diffusion, rearrangement and hydrogen atom abstraction, while k_{cat}[LA] is solely limited by hydrogen abstraction (17). However, at high temperature both k_{cat}/K_m[LA] and k_{cat}[LA] are solely limited by hydrogen abstraction. 15-hLO-1 has a similar kinetic behavior, with k_{cat}/K_m[LA] having multiple RDS's at low temperature (rearrangement and abstraction), but becoming solely limited by abstraction at high temperature. The k_{cat}[LA] is solely limited by abstraction at all temperatures (18). These results prompted the question of whether this similarity in kinetics between sLO-1 and 15-hLO-1 was maintained with AA as the substrate.

Our laboratories subsequently synthesized AA, di-deuterated on C-13 (13,13-d_2-AA), and determined for sLO-1 that the $^{D}k_{cat}$ with AA was similar to that with LA (19). A large $^{D}k_{cat}$[AA] was observed with small activation energies, indicating a similar tunneling mechanism for the hydrogen atom abstraction of both substrates. Moreover, the extent of diffusion control on the k_{cat}/K_m[AA] was at a maximum at 20 °C, decreasing in prominence as temperature increased or decreased, comparable to that of sLO-1 with LA as substrate (17). In contrast, the $^{D}k_{cat}/K_m$[AA] for sLO-1 was shown to be small (~8) and temperature independent, with no solvent isotope effect (SIE) at any temperature. These sLO-1 results with AA are distinct from the LA kinetics and can be best explained by an increase in affinity for AA, which results in an increase in commitment, and a subsequent decrease in $^{D}k_{cat}/K_m$[AA] (19).

For 15-hLO-1, it was determined using product branching experiments with d_4-AA, that the $^{D}k_{cat}$[AA] was small in comparison to the $^{D}k_{cat}$[AA] for sLO-1, with a value of 11.6 ± 2.0 for C13 and 8.5 ± 4.0 for C10 hydrogen atom abstraction (20). These values were in the range of semi-classical kinetic isotope effects and raised the possibility that the hydrogen atom abstraction for 15-hLO-1 with AA was not proceeding through a tunneling mechanism, opposite from that of LA. This potential difference between the catalytic mechanism of AA and LA for 15-hLO-1 is intriguing because it was recently observed that substrate specificity of 15-hLO-1 with AA and LA could be changed through product regulation of an allosteric site (13). If the mechanisms of catalysis for AA and LA are fundamentally different, then it is conceivable that this could help explain the change in substrate specificity of 15-hLO-1 and provide a method for investigating the effect of the allosteric site. In order to investigate this possibility further, we determined the primary kinetic isotope effect and the solvent isotope effect for both 15-hLO-1 and 12-hLO, with AA as substrate.

Material and Methods

Materials

All commercial fatty acids (Sigma-Aldrich Chemical Company) and LO products were re-purified using a Higgins HAIsil Semi-Preparative (5μm, 250 × 10 mm) C-18 column. Solution A was 99.9% MeOH and 0.1% acetic acid; solution B was 99.9% H_2O and 0.1% acetic acid. An isocratic elution of 85% A:15% B was used to purify all fatty acids, which were stored at −80 °C for a maximum of 6 months. Perdeuterated LA (d_{31}-LA) (98% deuterated, Cambridge Isotope Labs) was purified as previously described (21). The (10,10,13,13)-d_4-AA was synthesized as previously described (20,22,23). All other chemicals were reagent grade or better and were used without further purification.

Overexpression and Purification of 15-Human Lipoxygenase-1 and 12-Human Lipoxygenase

Human reticulocyte 15-lipoxygenase-1 (15-hLO-1) and human platelet 12-lipoxygenase (12-hLO) are N-terminally, His_6-tagged proteins, which were expressed and purified as previously published (24,25). All enzymes were purified to greater than 90% purity, as evaluated by SDS-PAGE analysis. Iron content of 12-hLO and 15-hLO-1 were determined with a Finnigan inductively coupled plasma mass spectrometer (ICP-MS), using cobalt-EDTA as an internal standard. Iron concentrations were compared to standardized iron solutions and used to normalize enzyme concentrations.

Steady-State Kinetic Measurements

Lipoxygenase rates were determined by following the formation of the conjugated diene product at 234 nm (ε = 25,000 M^{-1} cm^{-1}) with either a Perkin-Elmer Lambda 40 UV/Vis or a Cary 100 Bio spectrophotometer. All reactions were 2 mL in volume and constantly stirred using a magnetic stir bar at room temperature (22 °C) unless otherwise described. Assays were carried out in 25 mM Hepes buffer (pH 7.5) with substrate concentrations ranging from 1 μM – 20 μM, and were initiated by the addition of enzyme, as described below. The 12-hLO displays erratic behavior at low substrate concentrations (< 1 μM), resulting in large errors in the K_m values. To circumvent this inherent problem, we determined that adding the 12-hLO first, and then quickly initiating the reaction with the addition of the appropriate amount of substrate, yielded significantly more reproducible results. Substrate concentrations were quantitatively determined by allowing the enzymatic reaction to go to completion. Kinetic data were obtained by recording initial enzymatic rates at each substrate concentration and were then fitted to the Michaelis-Menten equation using the KaleidaGraph (Synergy) program to determine k_{cat} and k_{cat}/K_m values.

Determination of Kinetic Isotope Effect for 15-hLO-1 with AA as Substrate

The non-competitive kinetic isotope effect on the k_{cat} ($^{D}k_{cat}$[AA]) and k_{cat}/K_m ($^{D}k_{cat}/K_m$[AA]) values was determined by comparing the steady-state kinetic results of protiated arachidonic acid with that of d_4-arachidonic acid as previously described (17,18). Kinetic measurements were performed using a Cary 100 Bio spectrophotometer by following product formation at 234 nm, at temperatures ranging from 15 – 40 °C in 25 mM Hepes buffer at pH 7.5. Reactions were initiated using ~16 nM and ~40 nM (normalized to iron content) of 15-hLO-1 for protiated and deuterated arachidonic acid, respectively, with substrate concentrations ranging from 1–15 μM. Reactions were performed in the presence of purified 13-HPODE (~6 μM) (or 15-HPETE ~6 μM) to activate 15-hLO-1 and remove the kinetic lag phase. Kinetic parameters were determined as described in the steady-state kinetic section.

Determination of Kinetic Isotope Effect for 12-hLO with AA as Substrate

The non-competitive kinetic isotope effect on the k_{cat} ($^{D}k_{cat}$[AA]) and k_{cat}/K_m ($^{D}k_{cat}/K_m$[AA]) values was determined as described above for 15-hLO-1. The steady-state KIE experiments were performed using a PE Lambda 40 spectrophotometer, using buffer conditions described above (25 mM Hepes, pH 7.5) at temperatures ranging from 15 – 40 °C. Reactions were initiated using ~5 nM and ~60 nM (normalized to iron content) of 12-hLO for protiated and deuterated arachidonic acid, respectively, with substrate concentrations ranging from 0.1 – 10 μM. All kinetic parameters were determined as described in the steady-state kinetic section.

Determination of Solvent Isotope Effect for 12-hLO and 15-hLO-1 with AA as Substrate

The solvent isotope effect was determined by comparing the steady-state kinetic results of assays performed in H_2O and D_2O under temperatures ranging from 15 – 40 °C as previously described (17,18). Reactions were performed in 25 mM Hepes buffer at pH = 7.5 (pH meter reading was 7.1 for buffered D_2O), and initiated using ~5 nM and ~7 nM enzyme concentration (normalized to iron content), for 12-hLO and 15-hLO-1 respectively. All kinetic parameters were determined as described in the steady-state kinetic section. The variable-temperature SIE experiments for 15-hLO-1 included the addition of 13-HPODE (6 μM) to remove the kinetic lag phase. In addition, the SIE was performed with and without 12-HETE (5μM) at 15 °C, to determine if allosteric product binding affected the solvent dependency of the reaction.

Determining the Effects of 12-HETE on the Competitive Kinetic Isotope Effect and the Solvent Isotope Effect of 15-hLO-1 with AA as Substrate

The $^{D}k_{cat}/K_m$[AA] ratio was determined similarly to the previously published competitive substrate specificity method (13), which utilizes a Finnigan LTQ liquid chromatography - tandem mass spectrometer (LC-MS/MS) to quantify the product turnover. The enzymatic reactions were initiated by the addition of 1 μM substrate, of a known molar ratio (1:1) of d_4-AA:AA, with and without pre-incubation of 12-HETE (5 μM) (or 13-HODE, 5 μM) with 15-hLO-1 (~4 nM). Enzymatic assays were performed using buffer conditions described above (25 mM Hepes, pH 7.5, 22 °C). A Phenomenex Synergi Hydro-RP (4 μm, 150 × 2.0 mm) column was used to detect the reduced LO products with an elution protocol consisting of 0.2 ml/min, isocratic mobile phase of 59.9% ACN:40% H_2O:0.1% THF. The corresponding reduced product ion peak ratio was determined using negative ion MS/MS (collision energy = 35 eV), with the following masses; 15-HETE, parent m/z = 319, fragments m/z = 175 and 219, 12-HETE, parent m/z = 319, fragments m/z = 179 and 257, 13-HODE, parent m/z = 295, fragments m/z = 183 and 251, and perdeuterated 13-HODE, parent m/z = 325, fragments m/z = 213 and 281 (26). All extracted reaction mixtures were reduced with trimethylphosphite for LC-MS/MS analysis.

The effect of 12-HETE on the SIE of 15-hLO-1 was performed as described above; however, 12-HETE (5 μM) was added to each substrate concentration for steady-state kinetic analysis. Reactions were performed in 25 mM Hepes buffer (15 °C) at pH = 7.5 (pH meter reading was 7.1 for D_2O), and initiated using ~40 nM enzyme (normalized to iron content) of 15-hLO-1.

Reaction Rates at Varying O_2 Concentrations

Reaction rates of 15-hLO-1 with AA and LA were determined by measuring the extent of oxygen consumption on a Clark oxygen monitor as previously described (27). Reactions were carried out as a function of oxygen concentrations in 1 ml solutions, which were stirred constantly and equilibrated under air at 25 °C (258 μM O_2). The reaction was initiated by addition of ~30 nM 15-hLO-1 (normalized to iron content), via a gastight Hamilton syringe to the reaction chamber. The experiments were repeated at variable concentrations of oxygen, established by passing mixtures of N_2 and O_2 over stirred solutions in the reaction chamber

for 10 min. The established oxygen concentration was calibrated against the value of O_2 dissolved in an air-saturated solution at 25 °C (258 μM O_2). The rate of oxygen consumption was recorded at oxygen concentrations ranging from 5 - 500 μM, in 25 mM Hepes pH 7.5 (25 °C) and saturating conditions of substrate (25 μM). Further investigations were performed in the presence of the 12-HETE (5 μM), to determine if allosteric binding affected the $K_m(O_2)$, with either substrate.

Lag Phase Investigations of 15-hLO-1

Observations that 15-hLO-1 has an extended lag phase (activation period) with AA compared to LA prompted us to investigate if this effect is due to differences in their affinity towards the ferrous enzyme, as previously seen with sLO-1 (19). Reactions were carried out as described for the steady-state experiments (25 mM Hepes. pH 7.5, 22 °C), with the assays being initiated by 15-hLO-1, with 12 nM and 18 nM (normalized to iron content) for LA and AA, respectively, at substrate-limiting conditions (5 μM). The 15-hLO-1 enzyme was pre-incubated with AA (25 μM), followed by addition of LA, and vice versa, to determine the effect on the lag phase, as previously described (19).

Results and Discussion

Mechanistic Investigations of Human 15-Lipoxygenase-1 with AA as Substrate

Non-Competitive Kinetic Isotope Effect—Previous variable-temperature KIE studies with LO isozymes were limited to deuterated linoleic acid (17,18,21), since appropriately deuterated AA is not commercially available and is difficult to synthesize. In the current study, (10,10,13,13)-d_4-arachidonic acid (d_4-AA) was synthesized as previously described (20,22, 23), and utilized to investigate the primary KIE of 15-hLO-1 and 12-hLO. Deuterium labeling at both C10 and C13 was required to prevent changes in regioselectivity (20). Investigations of 15-hLO-1 with LA have previously demonstrated a temperature dependent $^{D}k_{cat}/K_m$[LA] and k_{cat}/K_m[LA] SIE, and a temperature independent $^{D}k_{cat}$[LA] (~40) and k_{cat}[LA] SIE (18). These studies suggest 15-hLO-1 displays hydrogen atom tunneling and has multiple RDSs at low temperature for k_{cat}/K_m[LA], whereas the k_{cat}[LA] is solely rate-limited by hydrogen atom abstraction. In the current work, the non-competitive, variable-temperature KIE of 15-hLO-1 with AA was significantly different, demonstrating temperature dependency for both $^{D}k_{cat}/K_m$[AA] and $^{D}k_{cat}$[AA] and with markedly lower magnitudes (Figure 1). The $^{D}k_{cat}/K_m$[AA] was determined to be 6.3 ± 2.5, 6.0 ± 1.5, 9.0 ± 1.6, 10.0 ± 2.3, 3.6 ± 1.5, 4.5 ± 2.0, for 15 °C, 20 °C, 25 °C, 30 °C, 35 °C and 40 °C, respectively. The $^{D}k_{cat}$[AA] data was determined to be 6.7 ± 0.6, 8.6 ± 0.6, 8.9 ± 1.1, 10.3 ± 0.7, 8.9 ± 1.4, 6.6 ± 0.9, for 15 °C, 20 °C, 25 °C, 30 °C, 35 °C and 40 °C, respectively. The change in $^{D}k_{cat}/K_m$[AA] and $^{D}k_{cat}$[AA] with respect to temperature is suggestive of multiple rate-limiting steps, as seen for 15-hLO-1 with LA; however, unlike with LA, the $^{D}k_{cat}/K_m$[AA] and $^{D}k_{cat}$[AA] values rise and then decrease at temperatures above 30 °C. In addition, the magnitude of both $^{D}k_{cat}/K_m$[AA] and $^{D}k_{cat}$[AA] for 15-hLO-1 are considerably smaller than the previously reported $^{D}k_{cat}/K_m$[LA] and $^{D}k_{cat}$[LA] values for 15-hLO-1 (18). The current values are within the range predicted by semi-classical mechanics (28,29) and suggest that possibly hydrogen atom tunneling does not occur. This hypothesis is difficult to confirm with ΔE_{act} and A_H/A_D investigations, as was reported for sLO-1 and 15-hLO-1 with LA (18,30), due to multiple RDS's for the k_{cat}[AA] of 15-hLO-1 at low temperature (vide infra). Moreover, the observed inactivation of 15-hLO-1 with AA at high temperatures makes the energy of activation (E_{act}) and the Arrhenius prefactor (A) for d_4-AA unattainable.

The non-competitive variable-temperature KIE data for 15-hLO-1 with AA was performed in the presence of 13-HPODE (6 μM) to remove the kinetic lag phase, which is more pronounced with AA than LA. However, this raises the concern that binding of 13-HPODE to the allosteric

site could affect the KIE, as was seen with the addition of 12-HPETE/HETE to 15-hLO-1 and LA (13). The non-competitive KIE study was therefore performed in the presence of 15-HPETE (6 μM) (25 mM Hepes, pH 7.5, 25 °C), which demonstrated that addition of 15-HPETE afforded the same KIE results as with 13-HPODE added ($^{D}k_{cat}/K_m$[AA] = 11 ± 2 and $^{D}k_{cat}$[AA] = 7.3 ± 0.6).

Competitive Kinetic Isotope Effect—To confirm the unexpectedly low $^{D}k_{cat}/K_m$[AA] value of 15-hLO-1, the competitive $^{D}k_{cat}/K_m$[AA] was determined with a mixture of d_4-AA and AA at 22 °C, using the LC-MS/MS method previously described for substrate specificity studies (13). Using d_4-AA, the $^{D}k_{cat}/K_m$[AA] values were determined to be 8 ± 1 and 10 ± 2 for abstraction from C13 and C10, respectively (Figure S1, Supplemental Material). These values are in good agreement with the averaged, non-competitive data at both C13 and C10 and with the previously published $^{D}k_{cat}$[AA] values from product branching experiments (20). Considering that no product was added to the competitive experiments and yet the $^{D}k_{cat}/K_m$[AA] value was the same as the non-competitive results, with both 13-HPODE and 15-HPETE added, this indicates that there was no allosteric effect on the $^{D}k_{cat}/K_m$[AA] of 15-hLO-1 with these products. As mentioned above, the low KIE values suggest that the hydrogen atom abstraction does not proceed through a tunneling mechanism; however, the intrinsic KIE values could also be masked due to either a large kinetic commitment with AA as substrate or due to a decreased contribution of the abstraction step to the rate-limiting step (19,21). To this end, 12-HETE (5 μM) was added to the competitive reaction mixture of d_4-AA/AA with 15-hLO-1 and the observed $^{D}k_{cat}/K_m$[AA] increased from 8 ± 1 to 18 ± 3, indicating that tunneling is involved in the hydrogen atom abstraction process. A similar result was previously observed with the addition of 12-HPETE or 12-HETE to 15-hLO-1, with $^{D}k_{cat}/K_m$[LA] increasing from 24 to 44 (13). 13-HODE was also added to the competitive peroxidation of d_4-AA/AA by 15-hLO-1 and was shown to have little effect on $^{D}k_{cat}/K_m$[AA] (10 ± 2), confirming the non-competitive KIE result (vide supra).

Solvent Isotope Effect—It was previously shown that the reaction of 15-hLO-1 with LA (no 13-HPODE added), displayed a temperature dependent k_{cat}/K_m[LA] SIE, yet no SIE for k_{cat}[LA], indicating that k_{cat}/K_m[LA] is partially rate-limited by a solvent dependent step, while k_{cat}[LA] is not (18). In contrast, the results for 15-hLO-1 with AA (13-HPODE added) demonstrate a temperature dependent SIE for both k_{cat}/K_m[AA] and k_{cat}[AA] (Figure 2), indicating multiple rate-limiting steps at low temperature for both k_{cat}/K_m[AA] and k_{cat}[AA]. This observation is consistent with the $^{D}k_{cat}/K_m$[AA] and $^{D}k_{cat}$[AA] temperature dependence data. The observed SIE at lower temperatures also explains the decreased substrate KIE values at low temperature, as a solvent dependent step would partially mask the observed KIE of the hydrogen atom abstraction step, since abstraction is not fully rate-limiting. The SIE data, however, does not explain the decreasing KIE values at high temperature, since there is no SIE effect in this temperature range (vide infra).

As discussed above, the addition of 12-HETE increased the competitive $^{D}k_{cat}/K_m$[AA] to a magnitude well above semi-classical predictions, whereas 13-HPODE and 15-HPETE had little effect on the $^{D}k_{cat}/K_m$[AA]. The effect of 12-HETE on the reaction mechanism of 15-hLO-1 was investigated further by probing the SIE at low temperature (15 °C), where the SIE is greatest. It was determined that the addition of 12-HETE (5 μM) significantly lowered the SIE from 2.3 ± 0.2 to 1.4 ± 0.2 and 2.4 ± 0.3 to 1.4 ± 0.2 for k_{cat}/K_m[AA] and k_{cat}[AA], respectively. This indicates that the solvent-dependent step for 15-hLO-1 has become less rate-limiting with the addition of 12-HETE, and corroborates the competitive $^{D}k_{cat}/K_m$[AA] results that show a larger substrate KIE under the same conditions. No effect on SIE was observed with the addition of 13-HPODE.

Reaction Rate at Varying O_2 Concentration—Previously our laboratory performed O_2 dependency experiments for the peroxidation of LA by 15-hLO-1 and AA by 12-hLO, and determined the $K_m(O_2)$ values to be 4.2 ± 1.1 μM and 7.0 ± 1.4 μM, respectively ([Substrate] = 25 μM, at 25 °C) (18). In the current investigation, 15-hLO-1 was studied with AA and LA (25 °C) concurrently, for direct comparison, and $K_m(O_2)$[LA] was determined to be 9.8 ± 0.7 μM and $K_m(O_2)$[AA] to be 25 ± 6 μM, indicating a 2.5-fold difference in the $K_m(O_2)$ between the two substrates (Table 1). The k_{cat} values were determined to be 7.6 ± 0.1 s^{-1} and 5.6 ± 0.3 s^{-1} for LA and AA, respectively, and are in agreement with k_{cat} values determined pectrophotometrically (13). The $k_{cat}/K_m(O_2)$ values were therefore determined to be 0.78 ± 0.07 $s^{-1}\mu M^{-1}$ and 0.23 ± 0.07 $s^{-1}\mu M^{-1}$ for LA and AA, respectively, indicating a greater than 3-fold preference for LA, in oxygen limiting conditions. The addition of 12-HETE (5 μM) demonstrated a decrease in the $k_{cat}/K_m(O_2)$ for LA (0.30 ± 0.07 $s^{-1}\mu M^{-1}$) and an increase in the $k_{cat}/K_m(O_2)$ for AA (0.32 ± 0.040 $s^{-1}\mu M^{-1}$), yielding similar $k_{cat}/K_m(O_2)$ values for the two substrates (Table 1). This is a remarkable result since the binding of 12-HETE to the allosteric site not only increases the fatty acid $(k_{cat}/K_m)^{AA}/(k_{cat}/K_m)^{LA}$ ratio 4-fold (13), but it also increases the oxygen $(k_{cat}/K_m)^{AA}/(k_{cat}/K_m)^{LA}$ ratio 3-fold. In both cases, 12-HETE increases the substrate specificity of 15-hLO-1 towards AA. The k_{cat} values with the addition of 12-HETE were determined to be 6.6 ± 0.3 s^{-1} and 5.2 ± 0.1 s^{-1} for LA and AA, respectively, and are in agreement with the previously published spectroscopic data (13).

Lag Phase Investigations—As mentioned, AA demonstrates higher affinity towards the ferrous sLO-1 enzyme than that of LA, manifested by a difference in their lag phase (19). This observation indicated that AA had a smaller K_D than LA, increasing commitment with AA, thereby lowering the observed $^{D}k_{cat}/K_m$[AA]. As seen in Figure 3, 15-hLO-1 also displays a longer lag phase with AA than LA, at low substrate concentrations. Pre-incubation of 15-hLO-1 with AA (25 μM) followed by LA (5 μM) addition, drastically extends the lag phase of the enzyme, whereas little effect is seen on the lag phase under the reverse conditions (pre-incubation with LA (25 μM) followed by AA (5 μM) addition). These data suggest that the affinity of AA to the ferrous 15-hLO-1 is greater than 5-fold that of LA, since 5 μM AA out-competes the binding of pre-incubated 25 μM LA, such that no reduction in the lag phase is seen. The LO products, 13-HPODE and 12-HPETE, were shown to eliminate the lag phase for 15-hLO-1 with AA, but the reduced products, 13-HODE and 12-HETE, did not affect the lag phase. Finally, there is no auto-inactivation of 15-hLO-1 with either AA or LA at low substrate concentration. However, at high substrate concentrations, AA auto-inactivates 15-hLO-1 to a much greater extent, as seen by the lower overall product production. This difference may be relevant for cellular processes since the low substrate concentration is more similar to that in the cell.

Summary of 15-hLO-1—Kinetic investigations of lipoxygenase center around the primary KIE of hydrogen atom abstraction since it is the first irreversible step for fatty acid kinetics. With this in mind, the general method for LO kinetic studies is to determine if the observed KIE can be dependent on multiple rate-limiting steps, as seen by temperature, solvent and viscogen dependencies or by masking of the observed KIE by a large commitment (vide infra). Invariably, the observed KIE is affected by a combination of these processes and this specific study strives to differentiate between the relative influence of these processes in the oxidation of AA by 15-hLO-1. In the current investigation, our laboratories have applied this method to probing 15-hLO-1 with AA as its substrate and demonstrated that the kinetics of 15-hLO-1 with AA are remarkably different from the kinetics with LA as substrate (18). The $^{D}k_{cat}$[AA] and $^{D}k_{cat}/K_m$[AA] values are small and slightly temperature dependent, with decreasing $^{D}k_{cat}/K_m$[AA] and $^{D}k_{cat}$[AA] values at both low and high temperature. At low temperature, the decrease in $^{D}k_{cat}/K_m$[AA] and $^{D}k_{cat}$[AA] is due to multiple RDS's (rearrangement and abstraction), as seen by an increasing SIE. However, at high temperature,

no SIE was observed for either k_{cat}/K_m or k_{cat}, indicating rearrangement is not responsible for the decrease in $^{D}k_{cat}/K_m$[AA] and $^{D}k_{cat}$[AA]. This decrease could be due to inactivation of 15-hLO-1 at high temperature or because diffusion is a rate-determining step (RDS). Unfortunately, the diffusion step cannot be investigated because the available viscogens affect catalysis (18). These results are distinct from the 15-hLO-1/LA kinetic results, in that both k_{cat}/K_m and k_{cat} for 15-hLO-1/AA are sensitive to rearrangement (SIE), and that the values of $^{D}k_{cat}/K_m$[AA] and $^{D}k_{cat}$[AA] are lower than a tunneling mechanism would predict (28,29). This latter issue was probed further by investigating the lag phase of 15-hLO-1. Previously, our laboratories postulated that the $^{D}k_{cat}/K_m$[AA] for sLO-1 was masked by a large commitment (k_2/k_{-1}, vide infra), since AA appeared to bind more tightly to the ferrous sLO-1 than LA, extending the lag phase (19). This experiment was repeated with 15-hLO-1 and it was observed that AA also extended the lag phase of LA catalysis. This result corroborates the hypothesis that AA binds more tightly to 15-hLO-1 than LA and thus has a larger commitment (k_2/k_{-1}). Commitment (k_2/k_{-1}) can be explained by examining the proposed mechanism of LO, minimally described by Scheme 2 (21,31,32).

$$\mathrm{KIE}={}^{D}k_{cat}/K_m=(k_{cat}/K_m)^{H}/(k_{cat}/K_m)^{D}=(k_2^{H}/k_2^{D}+k_2^{H}/k_{-1}^{H})/(1+k_2^{H}/k_{-1}^{H}) \quad (1)$$

According to Scheme 2, $^{D}k_{cat}/K_m$ would be defined by eq 1, where substrate release (k_{-1}) and hydrogen atom abstraction (k_2) are the primary determinants for $^{D}k_{cat}/K_m$ (this assumes $k_2 = k_{cat}$ and the multiple steps observed at low temperature are included in k_2). The $^{D}k_{cat}/K_m$ increases to a maximum of k_2^{H}/k_2^{D} when commitment (k_2/k_{-1}) is small, and decreases to a value approaching 1, when commitment for 15-hLO-1 with AA is large, assuming that the intrinsic k_2^{H}/k_2^{D} remains unchanged. Therefore, a large commitment for 15-hLO-1 with AA would lower the observed KIE and potentially mask a large intrinsic KIE, if tunneling were present.

This hypothesis was investigated further by adding the allosteric effector molecule, 12-HETE, which increased the observed $^{D}k_{cat}/K_m$[AA] from 8 to 18. This latter value is well above the semi-classical prediction and suggests that the hydrogen atom abstraction of AA by 15-hLO-1 is occurring through a tunneling mechanism. Nevertheless, the reason for the increase in the KIE is most likely not due to a change in commitment since addition of 12-HETE increases the k_{cat}/K_m[AA] but does not affect k_{cat}[AA] (13), indicating a decrease in K_m[AA]. Considering that the large commitment for 15-hLO-1 with AA is due to a small k_{-1}, it is unlikely that the observed decrease in K_m[AA] is due to an increase in k_{-1} and a subsequent decrease in commitment. In addition, it was observed that while 13-HPODE and 12-HPETE reduced the lag phase for 15-hLO-1 with AA, 13-HODE and 12-HETE did not. This indicated that the release rate for AA (k_{-1}), and hence commitment, was not changing upon allosteric binding.

The SIE of 15-hLO-1 was subsequently probed with the addition of 12-HETE to determine if the percent contributions of the rate-limiting steps were changing and the k_{cat}/K_m[AA] SIE was observed to decrease from 2.3 to 1.4. This result indicates that 12-HETE binding decreases the contribution of the solvent dependency on the rate-limiting step and subsequently increases the contribution of hydrogen atom abstraction for AA. The increase in contribution of hydrogen atom abstraction to the rate-limiting step would therefore increase the observed KIE, as is seen experimentally for AA. It should be noted that previously our laboratory demonstrated that 12-HETE increased the observed KIE for 15-hLO-1 with LA (13) and we postulated that the increase was due to a decrease in commitment, as seen by the decrease in k_{cat}[LA] (i.e. k_2). Nevertheless, given the current data, it is possible that the solvent dependent step could be affected as well. It should be noted that the change in $^{D}k_{cat}/K_m$ upon addition of 12-HETE could also be due to a change in the intrinsic k_2^{H}/k_2^{D}, but this can not be probed using the

temperature dependency of k_{cat}, as previously done for sLO-1 and 15-hLO-1 with LA (*18*, 30), since k_{cat} for 15-hLO-1 with AA is not fully rate-limited by hydrogen atom abstraction, and 15-hLO-1 auto-inactivates at high temperatures with AA. Interestingly, 13-HPODE does not increase the $^{D}k_{cat}/K_m$[AA] nor does it decrease the SIE, even though it has an allosteric effect on substrate specificity, similar to 12-HETE. This result suggests that 12-HETE and 13-HPODE affect the microscopic rate constants differently upon binding to the allosteric site.

The competitive $^{D}k_{cat}/K_m$[AA] for hydrogen atom abstraction from C13 is comparable to that for abstraction from C10, which corroborates the $^{D}k_{cat}$[AA] data previously determined (20). This result suggests that the hydrogen atom abstraction at these two structurally distinct positions is of a comparable mechanism. This is an unexpected result since the active site would have to spatially accommodate these two disparate positions for the same hydrogen atom abstraction process. Further investigations are in progress to probe this further.

Another difference between 15-hLO-1 kinetics with AA and LA is the difference in their $k_{cat}/K_m(O_2)$ values, and the differential effect of the allosteric effector molecule, 12-HETE. The $k_{cat}/K_m(O_2)$ for AA is over 3-fold less than that of LA, suggesting LA binds in a preferred conformation for dioxygen attack. This result is similar to that seen for the $k_{cat}/K_m(O_2)$ of sLO-1 with AA, which is over 9-fold less than that for LA (under saturating conditions of 13-HPODE) (33). The addition of 12-HETE raises the $k_{cat}/K_m(O_2)$ value of 15-hLO-1 with AA and decreases the $k_{cat}/K_m(O_2)$ value for LA, such that their $k_{cat}/K_m(O_2)$ values become equivalent for both substrates. These results indicate that upon allosteric binding, either the position of the substrate relative to the O_2 channel has changed or that the O_2 channel itself has changed. This result may be relevant for human disease models since the oxygen concentration varies from 20 μM in normal tissue (34), to as low as 6 μM in prostate cancer (35), and hence oxygen concentration could regulate LO substrate specificity in the cell.

Mechanistic Investigations of Human 12-Lipoxygenase with AA as Substrate

Non-Competitive Kinetic Isotope Effect—Variable-temperature KIE experiments demonstrated that the $^{D}k_{cat}/K_m$[AA] and $^{D}k_{cat}$[AA] of 12-hLO were temperature dependent, with values ranging from 4.7 ± 0.9 to 48 ± 15 and 5.5 ± 0.6 to 22 ± 4 between 15 °C and 40 °C, respectively (Figure 4).

The magnitude of both $^{D}k_{cat}/K_m$[AA] and $^{D}k_{cat}$[AA], at high temperature, are indicative of hydrogen atom tunneling, as previously seen for 15-hLO-1 with LA (18). The value of $^{D}k_{cat}/K_m$[AA] at high temperature does not match with the value of $^{D}k_{cat}$[AA], which could be due to the inactivation of 12-hLO, as seen by the increased error, and is similar to that seen for 15-hLO-1 with LA (18). The temperature dependence of both $^{D}k_{cat}/K_m$[AA] and $^{D}k_{cat}$[AA] for 12-hLO is indicative of multiple RDS's in the reaction mechanism that contribute differently to the overall rate at the different temperatures.

Solvent Isotope Effect—Previously, our laboratory determined that 12-hLO displayed a temperature dependent SIE for k_{cat}[AA], but a temperature independent k_{cat}/K_m[AA] SIE, albeit with a large degree of error (18). However, in the current study 12-hLO displayed a temperature dependent KIE for both $^{D}k_{cat}/K_m$[AA] and $^{D}k_{cat}$[AA], suggesting a possible discrepancy between these two results. Considering that the original SIE data (18) and the current KIE data were performed under different conditions (25 mM Tris, pH 7.5 versus 25 mM Hepes, pH 7.5, respectively), the SIE experiments were re-examined using the KIE reaction conditions of this investigation. Under these new conditions, the error was reduced considerably and the solvent isotope effect for 12-hLO at pD 7.1 (pH 7.5) was determined to be approximately 1.4 at 15 °C, decreasing with increasing temperature to approximately 1.0, for both the k_{cat}/K_m[AA] and k_{cat}[AA] (Figure 5). The new SIE data correlates well with the

substrate KIE data, providing further support for multiple rate-limiting steps at low temperature for both k_{cat}/K_m[AA] and k_{cat}[AA].

Temperature dependency of hydrogen atom abstraction—Considering that there are multiple RDS's for the k_{cat}[AA] of 12-hLO at low temperature, it is not possible to determine the ΔE_{act} and A_H/A_D, as previously determined for sLO-1 and 15-hLO-1 with LA (18,30). Nevertheless, the energy of activation (E_{act}) and the Arrhenius prefactor (A) for the d_4-AA can be estimated, since the peroxidation of deuterated substrate is most likely solely rate-limited by deuterium atom abstraction and there is no auto-inactivation at higher temperature, as seen for 15-hLO-1. Fitting the data with the empirical Arrhenius equation ($k = A \exp^{-E_{act}/RT}$), where R represents the gas constant, T is the absolute temperature, E_{act} is the energy of activation, and A is the Arrhenius prefactor (Figure 6), the E_{act} was determined to be 11.9 ± 1.0 kcal/mol and the A_D to be 4×10^8 s^{-1} (Table 2). In comparing the 12-hLO/d_4-AA data with the 15-hLO-1/d_{31}-LA data, one observes that their E_{act} values are much smaller than the predicted value of 76 kcal/mol for the pentadienyl C-H homolytic bond cleavage (36), that their A_D values are much smaller than the predicted Arrhenius prefactor ($A_{TST} \sim 10^{13}$ s^{-1}) from the semi-classical model (i.e. the bond-stretch model) (37), and that the magnitude of $^D k_{cat}/K_m$[AA] and $^D k_{cat}$[AA] at high temperature are much greater than semi-classical predictions (7-10) (28,29). These combined 12-hLO kinetic data are therefore consistent with a hydrogen tunneling mechanism (28).

These results demonstrate that not only is 12-hLO distinct from 15-hLO-1 in both its fatty acid metabolism (only reacting with AA) and its primary sequence (80% similar/65% identical), but also in its reaction mechanism with AA. Our data demonstrates that both $^D k_{cat}/K_m$ and $^D k_{cat}$ increase to large values at high temperature, whereas 15-hLO-1/AA KIE is at a maximum at 30 °C. However, the catalytic mechanism of 12-hLO is similar to that of 15-hLO-1 with AA in that its hydrogen atom abstraction proceeds through a tunneling mechanism, and both isozymes demonstrate a solvent dependent step for both k_{cat}/K_m and k_{cat}, at low temperature. Interestingly, the magnitude of the SIE value for 12-hLO is lower than that for 15-hLO-1, suggesting a smaller participation in the rate-limiting step. Unfortunately, it could not be determined if diffusion is also a rate-limiting step, as seen for sLO-1 with LA (17), since viscogens inhibit catalysis of 12-hLO (18). It should be noted that although both 15-hLO-1 and 12-hLO display a temperature dependent KIE due to multiple rate-limiting steps, which include hydrogen atom abstraction and a solvent dependent step, gating cannot be completely discounted as a factor. The environmentally coupled tunneling model predicts that even if hydrogen abstraction is the sole RDS, changes in the gating energy can lead to a slightly temperature dependent KIE (28-30). Since the k_{cat} of both enzymes are not fully rate-limited by hydrogen atom abstraction, this aspect of both 15-hLO-1 and 12-hLO catalysis could not be investigated.

Conclusion

In conclusion, this investigation illustrates four important properties of mammalian lipoxygenases. First, the general catalytic mechanism of 15-hLO-1/AA is similar to that of 12-hLO/AA with respect to both having multiple RDSs at low temperature (rearrangement and abstraction) and that the abstraction proceeds through a tunneling mechanism. However, the commitment (k_2/k_{-1}) of 15-hLO-1/AA is large enough, relative to its intrinsic KIE, to lower the observed $^D k_{cat}/K_m$[AA] significantly. Second, the $k_{cat}/K_m[O_2]$ with AA of 15-hLO-1 is over 3-fold higher compared to 12-hLO with AA, which could affect their relative activity in cells, where oxygen concentration is limited. Third, the binding of 12-HETE to the allosteric site of 15-hLO-1 lowers the solvent dependent step (SIE) such that hydrogen atom abstraction (KIE) becomes the predominant rate-limiting step, and increases the AA/LA ratio for $k_{cat}/K_m[O_2]$, such that there is no substrate preference between LA and AA, under limiting oxygen

concentrations. These results, as well as our previous discovery that 12-HETE affects the AA/LA ratio for k_{cat}/K_m[Fatty Acid], suggest that under cellular conditions, the allosteric binding of 12-HETE to 15-hLO-1 would increase its substrate specificity towards AA over LA, which may have important implications in cancer progression. Finally, it appears that hydrogen atom tunneling is a common feature in the lipoxygenase mechanism, despite the variations between the microscopic rate constants of the various LO isozymes (sLO-1, 15-hLO-1 and 12-hLO), with the two substrates (AA and LA).

Supplementary Material

Refer to Web version on PubMed Central for supplementary material.

References

1. Solomon EI, Zhou J, Neese F, Pavel EG. New insights from spectroscopy into the structure/function relationships of lipoxygenases. Chem Biol 1997;4:795–808. [PubMed: 9384534]
2. Nakano H, Inoue T, Kawasaki N, Miyataka H, Matsumoto H, Taguchi T, Inagaki N, Nagai H, Satoh T. Synthesis and biological activities of novel antiallergic agents with 5-lipoxygenase inhibiting action. Bioorg Med Chem 2000;8:373–80. [PubMed: 10722160]
3. Ghosh J, Myers CE. Inhibition of arachidonate 5-lipoxygenase triggers massive apoptosis in human prostate cancer cells. Proc Natl Acad Sci U S A 1998;95:13182–7. [PubMed: 9789062]
4. Steele VE, Holmes CA, Hawk ET, Kopelovich L, Lubet RA, Crowell JA, Sigman CC, Kellof GJ. Lipoxygenase Inhibitors as Potential Cancer Chemopreventives. Cancer Epidemiology, Biomarkers & Prevention 1999;8:467–483.
5. Hussain H, Shornick LP, Shannon VR, Wilson JD, Funk CD, Pentland AP, Holtzman MJ. Epidermis contains platelet-type 12-lipoxygenase that is overexpressed in germinal layer keratinocytes in psoriasis. Am J Physiol 1994;266:C243–53. [PubMed: 8304420]
6. Connolly JM, Rose DP. Enhanced angiogenesis and growth of 12-lipoxygenase gene-transfected MCF-7 human breast cancer cells in athymic nude mice. Cancer Lett 1998;132:107–12. [PubMed: 10397460]
7. Natarajan R, Nadler J. Role of lipoxygenases in breast cancer. Front Biosci 1998;3:E81–8. [PubMed: 9616130]
8. Harats D, Shaish A, George J, Mulkins M, Kurihara H, Levkovitz H, Sigal E. Overexpression of 15-lipoxygenase in vascular endothelium accelerates early atherosclerosis in LDL receptor-deficient mice. Arterioscler Thromb Vasc Biol 2000;20:2100–5. [PubMed: 10978255]
9. Kamitani H, Geller M, Eling T. Expression of 15-lipoxygenase by human colorectal carcinoma Caco-2 cells during apoptosis and cell differentiation. J Biol Chem 1998;273:21569–77. [PubMed: 9705287]
10. Shappell SB, Manning S, Boeglin WE, Guan YF, Roberts RL, Davis L, Olson SJ, Jack GS, Coffey CS, Wheeler TM, Breyer MD, Brash AR. Alterations in lipoxygenase and cyclooxygenase-2 catalytic activity and mRNA expression in prostate carcinoma. Neoplasia 2001;3:287–303. [PubMed: 11571629]
11. Butler R, M SH, Tindall DJ, Young CY. Nonapoptotic cell death associated with S-phase arrest of prostate cancer cells via the peroxisome proliferator-activated receptor gamma ligand, 15-deoxy-delta12,14-prostaglandin J2. Cell Growth Diff 2000;11:49–61. [PubMed: 10672903]
12. Hsi LC, Wilson L, Nixon J, Eling TE. 15-lipoxygenase-1 metabolites down-regulate peroxisome proliferator-activated receptor gamma via the MAPK signaling pathway. J Biol Chem 2001;276:34545–52. [PubMed: 11447213]
13. Wecksler AT, Kenyon V, Deschamps JD, Holman TR. Substrate specificity changes for human reticulocyte and epithelial 15-lipoxygenases reveal allosteric product regulation. Biochemistry 2008;47:7364–75. [PubMed: 18570379]
14. Brash AR, Boeglin WE, Chang MS. Discovery of a second 15S-lipoxygenase in humans. Proc Natl Acad Sci U S A 1997;94:6148–52. [PubMed: 9177185]
15. Kilty I, Logan A, Vickers PJ. Differential characteristics of human 15-lipoxygenase isozymes and a novel splice variant of 15S-lipoxygenase. Eur J Biochem 1999;266:83–93. [PubMed: 10542053]

16. Ruddat VC, Mogul R, Chorny I, Chen C, Perrin N, Whitman S, Kenyon V, Jacobson MP, Bernasconi CF, Holman TR. Tryptophan 500 and arginine 707 define product and substrate active site binding in soybean lipoxygenase-1. Biochemistry 2004;43:13063–71. [PubMed: 15476400]

17. Glickman MH, Klinman JP. Nature of rate-limiting steps in the soybean lipoxygenase-1 reaction. Biochemistry 1995;34:14077–92. [PubMed: 7578005]

18. Segraves EN, Holman TR. Kinetic investigations of the rate-limiting step in human 12- and 15-lipoxygenase. Biochemistry 2003;42:5236–43. [PubMed: 12731864]

19. Jacquot C, Peng S, van der Donk WA. Kinetic isotope effects in the oxidation of arachidonic acid by soybean lipoxygenase-1. Bioorg Med Chem Lett 2008;18:5959–62. [PubMed: 18793849]

20. Jacquot C, Wecksler AT, McGinley CM, Segraves EN, Holman TR, van der Donk WA. Isotope sensitive branching and kinetic isotope effects in the reaction of deuterated arachidonic acids with human 12- and 15-lipoxygenases. Biochemistry 2008;47:7295–303. [PubMed: 18547056]

21. Lewis E, Johnson E, Holman T. Large Competitive Kinetic Isotope Effects in Human 15-Lipoxygenase Catalysis Measured by a Novel HPLC Method. J Am Chem Soc 1999;121:1395–1396.

22. Peng S, Okeley NM, Tsai AL, Wu G, Kulmacz RJ, van der Donk WA. Synthesis of isotopically labeled arachidonic acids to probe the reaction mechanism of prostaglandin H synthase. J Am Chem Soc 2002;124:10785–96. [PubMed: 12207535]

23. Peng S, McGinley CM, van der Donk WA. Synthesis of site-specifically labeled arachidonic acids as mechanistic probes for prostaglandin H synthase. Org Lett 2004;6:349–52. [PubMed: 14748590]

24. Amagata T, Whitman S, Johnson TA, Stessman CC, Loo CP, Lobkovsky E, Clardy J, Crews P, Holman TR. Exploring sponge-derived terpenoids for their potency and selectivity against 12-human, 15-human, and 15-soybean lipoxygenases. J Nat Prod 2003;66:230–5. [PubMed: 12608855]

25. Chen XS, Brash AR, Funk CD. Purification and characterization of recombinant histidine-tagged human platelet 12-lipoxygenase expressed in a baculovirus/insect cell system. Eur J Biochem 1993;214:845–52. [PubMed: 8319693]

26. Deems R, Buczynski MW, Bowers-Gentry R, Harkewicz R, Dennis EA. Detection and Quantitation of Eicosanoids via High Performance Liquid Chromatography-Electrospray Ionization-Mass Spectrometry. Methods Enzymol 2007;432:59–82. [PubMed: 17954213]

27. Knapp MJ, Klinman JP. Kinetic studies of oxygen reactivity in soybean lipoxygenase-1. Biochemistry 2003;42:11466–75. [PubMed: 14516198]

28. Knapp MJ, Klinman JP. Environmentally coupled hydrogen tunneling. Linking catalysis to dynamics. Eur J Biochem 2002;269:3113–21. [PubMed: 12084051]

29. Klinman JP. The role of tunneling in enzyme catalysis of C-H activation. Biochim Biophys Acta 2006;1757:981–7. [PubMed: 16546116]

30. Knapp MJ, Rickert K, Klinman JP. Temperature-dependent isotope effects in soybean lipoxygenase-1: correlating hydrogen tunneling with protein dynamics. J Am Chem Soc 2002;124:3865–74. [PubMed: 11942823]

31. Mogul R, Johansen E, Holman TR. Oleyl sulfate reveals allosteric inhibition of soybean lipoxygenase-1 and human 15-lipoxygenase. Biochemistry 2000;39:4801–7. [PubMed: 10769137]

32. Ruddat VC, Whitman S, Holman TR, Bernasconi CF. Stopped-flow kinetic investigations of the activation of soybean lipoxygenase-1 and the influence of inhibitors on the allosteric site. Biochemistry 2003;42:4172–8. [PubMed: 12680771]

33. Peng S, van der Donk WA. An unusual isotope effect on substrate inhibition in the oxidation of arachidonic acid by lipoxygenase. J Am Chem Soc 2003;125:8988–9. [PubMed: 15369335]

34. Hudetz AG. Mathematical model of oxygen transport in the cerebral cortex. Brain Res 1999;817:75–83. [PubMed: 9889326]

35. Parker C, Milosevic M, Toi A, Sweet J, Panzarella T, Bristow R, Catton C, Catton P, Crook J, Gospodarowicz M, McLean M, Warde P, Hill RP. Polarographic electrode study of tumor oxygenation in clinically localized prostate cancer. Int J Radiat Oncol Biol Phys 2004;58:750–7. [PubMed: 14967430]

36. McMillen DF, G DM. Hydrocarbon Bond Dissociation Energies. Ann Rev Phys Chem 1982;33:493–532.

37. Kim Y, Kreevoy MM. The experimental manifestations of corner-cutting tunneling. Journal of the American Chemical Society 1992;114:7116–7123.

Abbreviations

LO	lipoxygenase
sLO-1	soybean lipoxygenase-1
15-hLO-1	human reticulocyte 15-lipoxygenase-1
12-hLO	human platelet 12-lipoxygenase
AA	arachidonic acid
15-HPETE	15-(S)-hydroperoxyeicosatetraenoic acid
15-HETE	15-(S)-hydroxyeicosatetraenoic acid
12-HPETE	12-(S)-hydroperoxyeicosatetraenoic acid
12-HETE	12-(S)-hydroxyeicosatetraenoic acid
d_4-AA	(10,10,13,13)-d_4-AA
LA	linoleic acid
d_{31}-LA	fully deuterated LA
13-HPODE	13-(S)-hydroperoxyoctadecadienoic acid
13-HODE	13-(S)-hydroxyoctadecadienoic acid
perdeuterated 13-HPODE	fully deuterated 13-(S)-HPODE
perdeuterated 13-HODE	fully deuterated 13-(S)-HODE
k_{cat}	the rate constant for product release
k_{cat}/K_m	the rate constant for substrate capture
$k_{cat}/K_m(O_2)$	the rate constant for oxygen binding, $^{D}k_{cat}/K_m$, primary kinetic isotope effect for k_{cat}/K_m
$^{D}k_{cat}$	primary kinetic isotope effect for k_{cat}

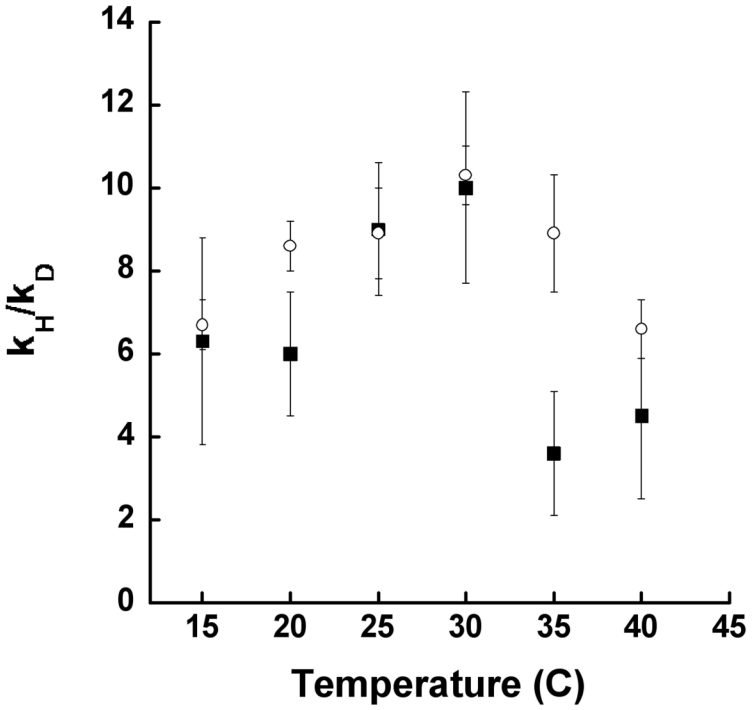

Figure 1.

Temperature dependence of the apparent primary k_H/k_D for 15-hLO-1: $^Dk_{cat}$ (open circles) and $^Dk_{cat}/K_m$ (closed squares). Enzymatic assays were performed in 25 mM Hepes buffer (pH 7.5) with 13-HPODE (6 μM) addition.

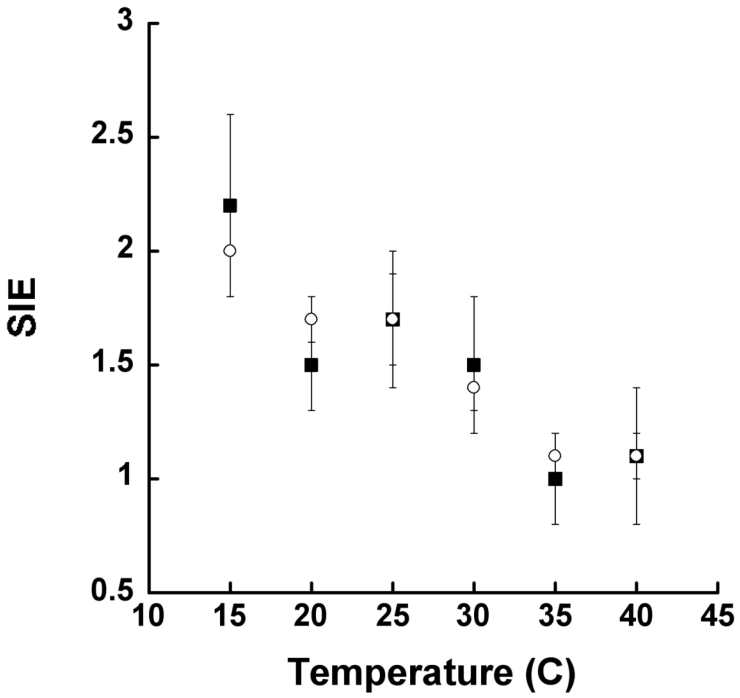

Figure 2.

Temperature dependence of solvent isotope effect for 15-hLO-1: k_{cat} (open circles) and k_{cat}/K_m (closed squares). Enzymatic assays were performed in 25 mM Hepes buffer (pH 7.5) with 13-HPODE (6 μM) addition.

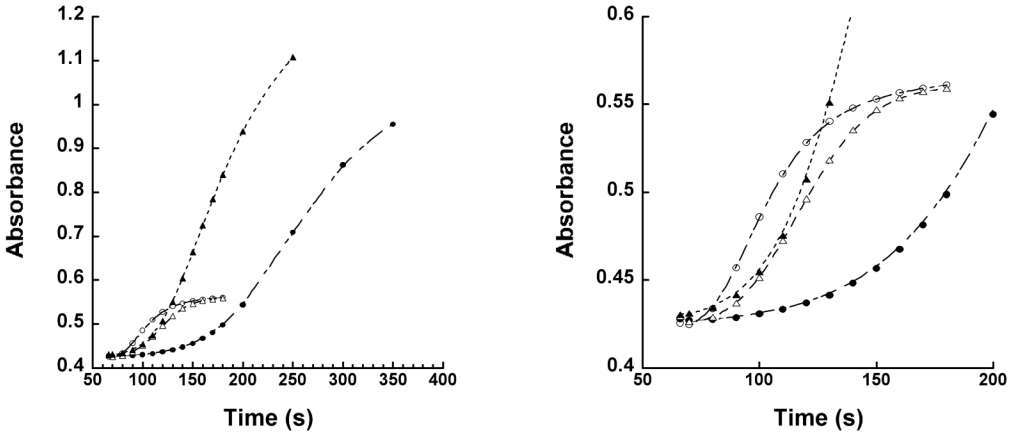

Figure 3.

Lag phase comparison of 15-hLO-1 with AA (5 μM) (open triangles) and LA (5 μM) (open circles). Pre-incubation with AA (25 μM) followed by LA (5 μM) addition (closed circles), and pre-incubation of LA (25 μM) followed by AA (5 μM) addition (closed triangles). Enzymatic assays were performed in 25 mM Hepes buffer (pH 7.5, 22 °C). Insert: Magnified view of lag phase data.

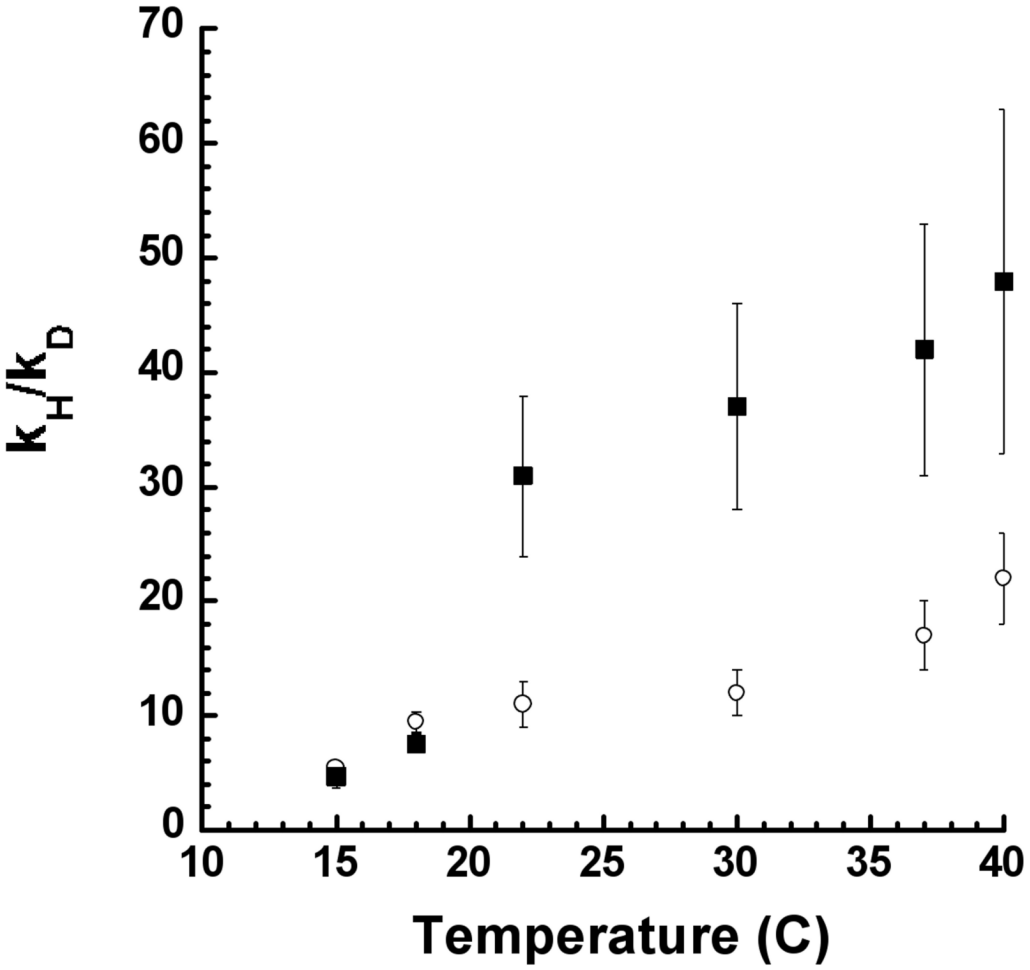

Figure 4.
Temperature dependence of apparent primary k_H/k_D for 15-hLO-1: $^{D}k_{cat}$ (open circles) and $^{D}k_{cat}/K_m$ (closed squares). Enzymatic assays were performed in 25 mM Hepes buffer (pH 7.5).

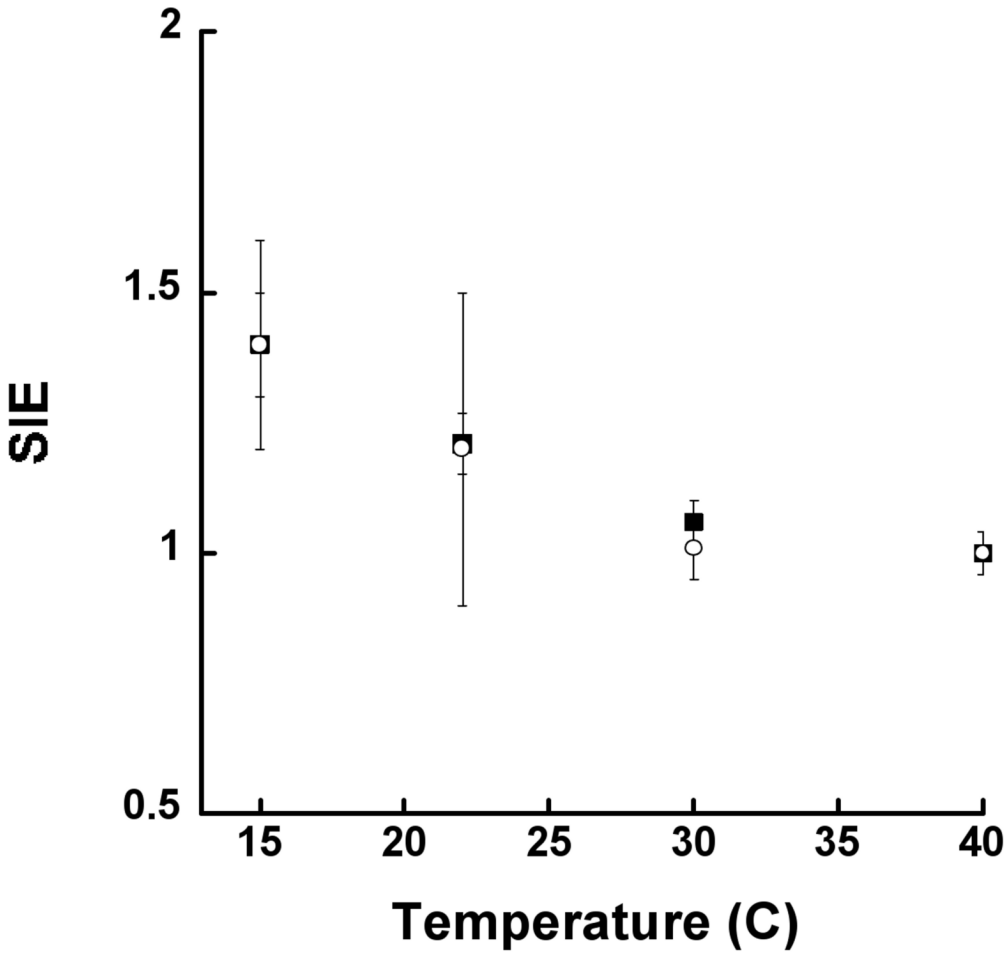

Figure 5.
Temperature dependence of solvent isotope effect 12-hLO: $^{D}k_{cat}$ (closed squares) and $^{D}k_{cat}/K_m$ (open circles). Enzymatic assays were performed in 25 mM Hepes buffer (pH 7.5).

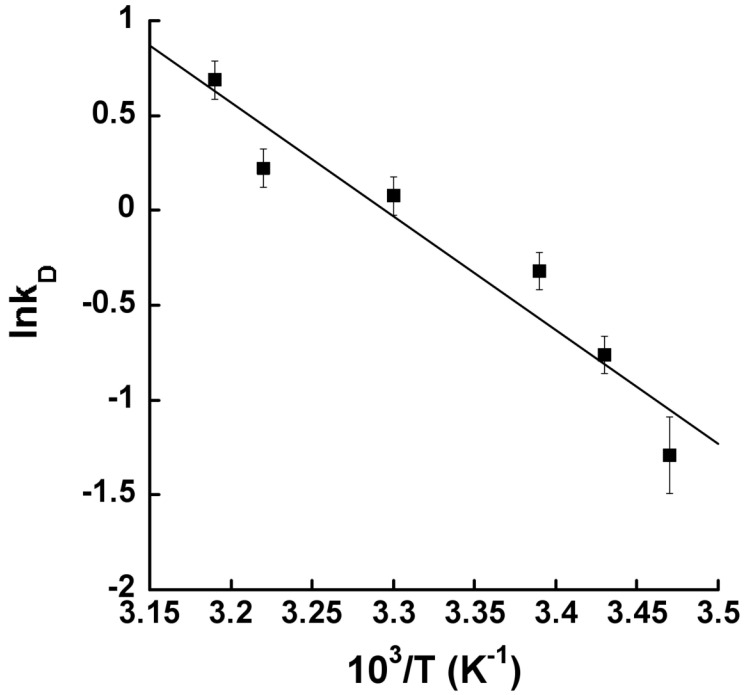

Figure 6.
Arrhenius plot of kinetic data for 12-hLO with d_4-AA. Nonlinear fit is shown as a solid line. Enzymatic assays were performed in 25 mM Hepes, pH 7.5.

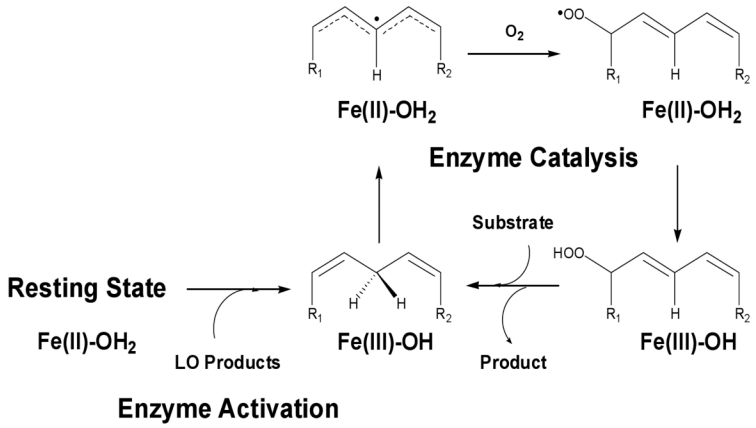

Scheme 1.

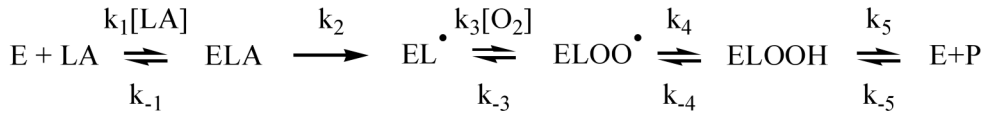

Scheme 2.

Table 1

Comparison of the Steady-State Kinetic Parameters of 15-hLO-1 for Oxygen with AA and LA as Substrates[a]

		No Product Addition	12-HETE Addition
AA			
	k_{cat}	5.6 ± 0.3	5.2 ± 0.1
	$K_m(O_2)$	25 ± 6	17 ± 2
	$k_{cat}/K_m(O_2)$	0.23 ± 0.07	0.32 ± 0.04
LA			
	k_{cat}	7.6 ± 0.1	6.6 ± 0.3
	$K_m(O_2)$	9.8 ± 0.7	22 ± 4
	$k_{cat}/K_m(O_2)$	0.78 ± 0.07	0.30 ± 0.07

[a] Enzymatic assays were performed in 25 mM Hepes buffer (pH 7.5, 25 °C), with and without product addition, in the presences of 25 μM substrate. Oxygen consumption was detected using a Clark oxygen monitor.

Table 2

Energy of Activation and Arrhenius Prefactors Determination for Human Lipoxygenase Deuterium Abstraction[a]

	Substrate	$^{D}k_{cat}$[b]	E_{act} (kcal/mol)	A_D (s^{-1})
12-hLO	AA	12.0 (2.0)	11.9 (1.0)	4×10^8
15-hLO-1	LA[c]	40.0 (8.0)	8.7 (0.2)	4×10^5

[a] Data were collected between 15 – 40 °C in 25 mM Hepes pH 7.5 for 15-hLO-1, and 25mM Tris pH 7.5 for 12-hLO.

[b] $^{D}k_{cat} = k_{cat}^{H}/k_{cat}^{D}$ at 30 °C.

[c] From previously published data (18).